

Air-Stable High-PLQY Cesium Lead Halide Perovskites for Laser-Patterned Displays

Ping Liu,^{1,2,#} Boyang Yu,^{3,#} Wanqing Cai,^{1,2,#} Xiongxian Yao,^{1,2} Kai Chang,³ Xinyan Zhao,³ Zhichun Si,² Weiwei Deng,^{3,*} Yuanyuan Zhou,^{4,5,*} Guangmin Zhou,^{1,2,*} and Guodan Wei^{1,2,*}

¹ Tsinghua-Berkeley Shenzhen Institute (TBSI), Tsinghua University, Shenzhen 518055, China

² Institute of Materials Science, Tsinghua Shenzhen International Graduate School, Tsinghua University, Shenzhen 518055, China

³ Department of Mechanics and Aerospace Engineering, Southern University of Science and Technology (SUSTech), Shenzhen 518055, China

⁴ Department of Applied Physics, The Hong Kong Polytechnic University, Hong Kong SAR, 999077, China

⁵ Smart Society Laboratory, Hong Kong Baptist University, Kowloon, Hong Kong SAR, 999077, China

These three authors are equally contributed.

* Email:

dengww@sustech.edu.cn; weiguodan@sz.tsinghua.edu.cn; yyzhou@hkbu.edu.hk;
guangminzhou@sz.tsinghua.edu.cn

Supporting Information

Table S1. Performance summary of colour-saturated pure red perovskite thin films.

Emission layer	Emission peak (nm)	PLQY(%)	Reference
ACDC-treated MAPbI ₂ Br NCs film	635	30	[1]
KBr passivated CsPbI _{3-x} Br _x NCs films	637	64	[2]
Cu ²⁺ -substituted CsPbBrI ₂ NCs film	630	81	[3]
BI-treated CsPb(Br/I) ₃ NCs film	625	76	[4]
EDTA and glutathione multidentate ligands treated MAPbI _x Br _{3-x} NCs film	620	68	[5]
PEO/quasi-2D perovskite film	638	60	[6]
PEA/NMA co-spacer quasi-2D perovskite film	635	51	[7]
2D (PEA) ₂ SnI ₄ film	629	1.52	[8]
2D (PEA) ₂ SnI ₄ film	640	7.1	[9]
PBABr–CsPbBr _{0.6} I _{2.4} -PEtOx	634	91	This work

Table S2. The statistical summary table of SEM and AFM corresponding parameters.

Sample	Mean grain size (nm)	Root-mean-square roughness (Ra, nm)
CsPbBr _{0.6} I _{2.4} control sample	152	9.83
PBABr/CsPbBr _{0.6} I _{2.4}	43	3.24
CsPbBr _{0.6} I _{2.4} /PEtOx	30	2.73
PBABr–CsPbBr _{0.6} I _{2.4} -PEtOx	34	2.75

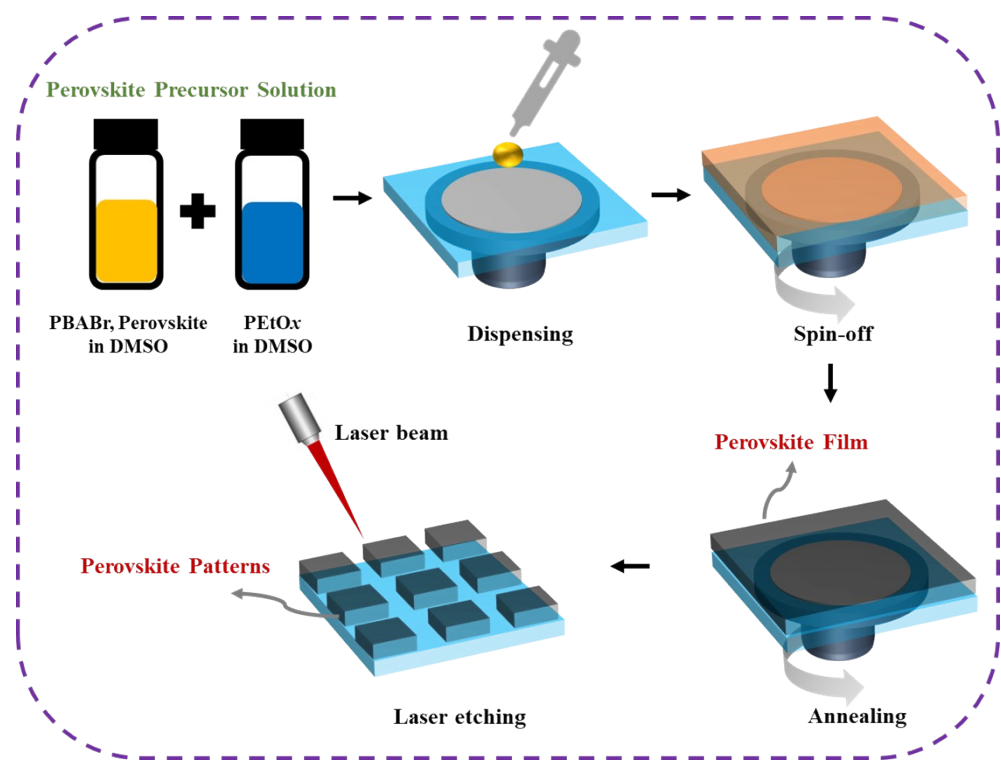


Figure S1. The processes of preparing direct laser etching patterning of light emitting PBABr/CsPbBr_{0.6}I_{2.4}/PEtOx composite thin films.

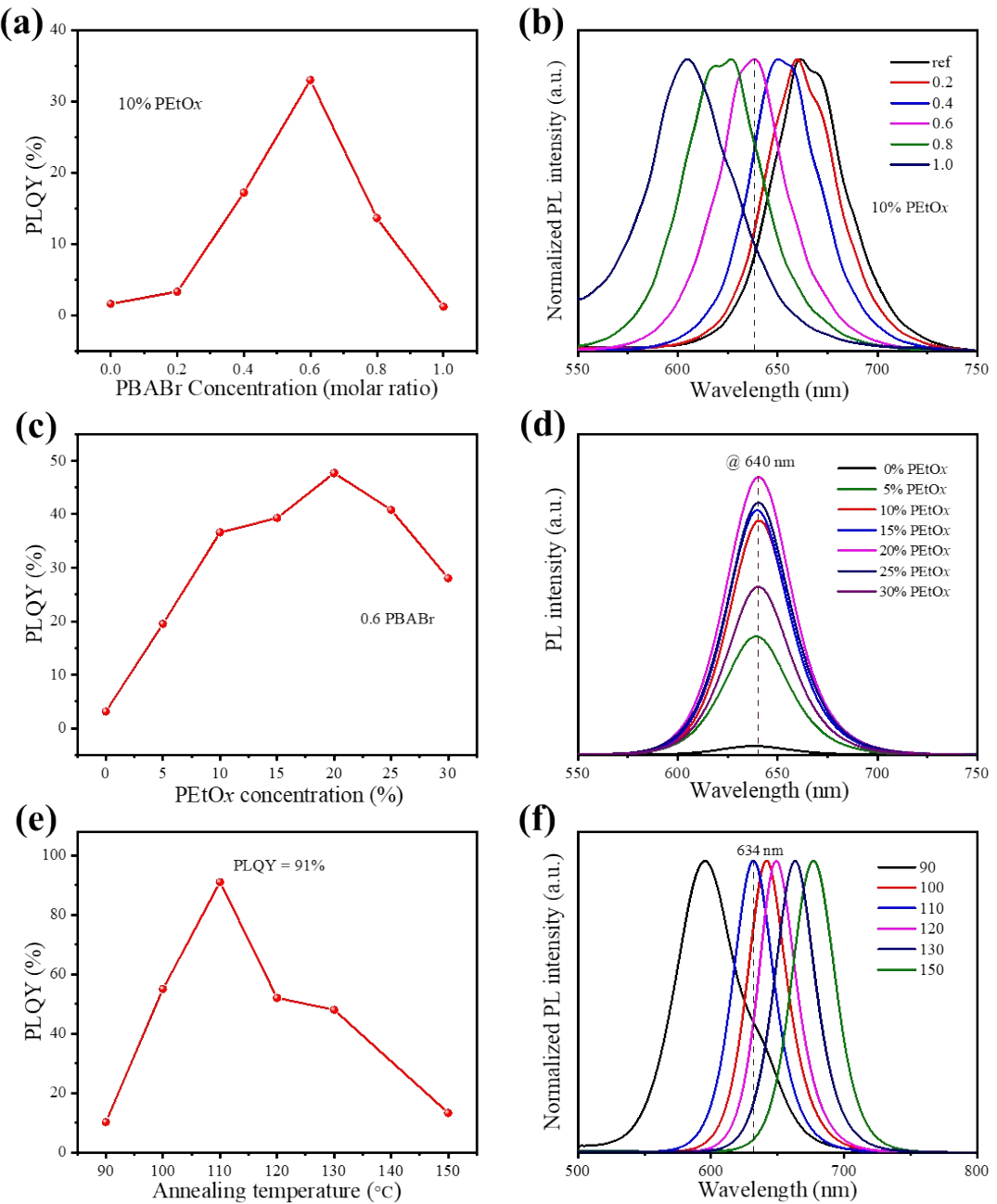


Figure S2. The details of the PLQY optimization of PBABr/CsPbBr_{0.6}I_{2.4}/PEtOx composite thin films. Experimental conditions: (a-b) PEtOx concentration is 10% and annealing temperature is 130 °C. (c-d) Molar ratio of PBABr is 0.6 and annealing temperature is 130 °C. (e-f) PEtOx concentration is 20% and molar ratio of PBABr is 0.6.

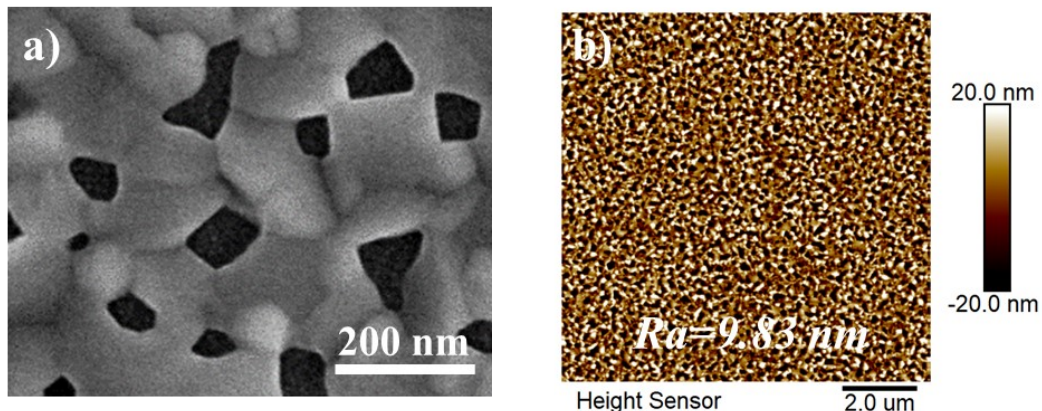


Figure S3. (a) SEM and (b) AFM images showing the surface morphologies of 3D $\text{CsPbBr}_{0.6}\text{I}_{2.4}$ control sample.

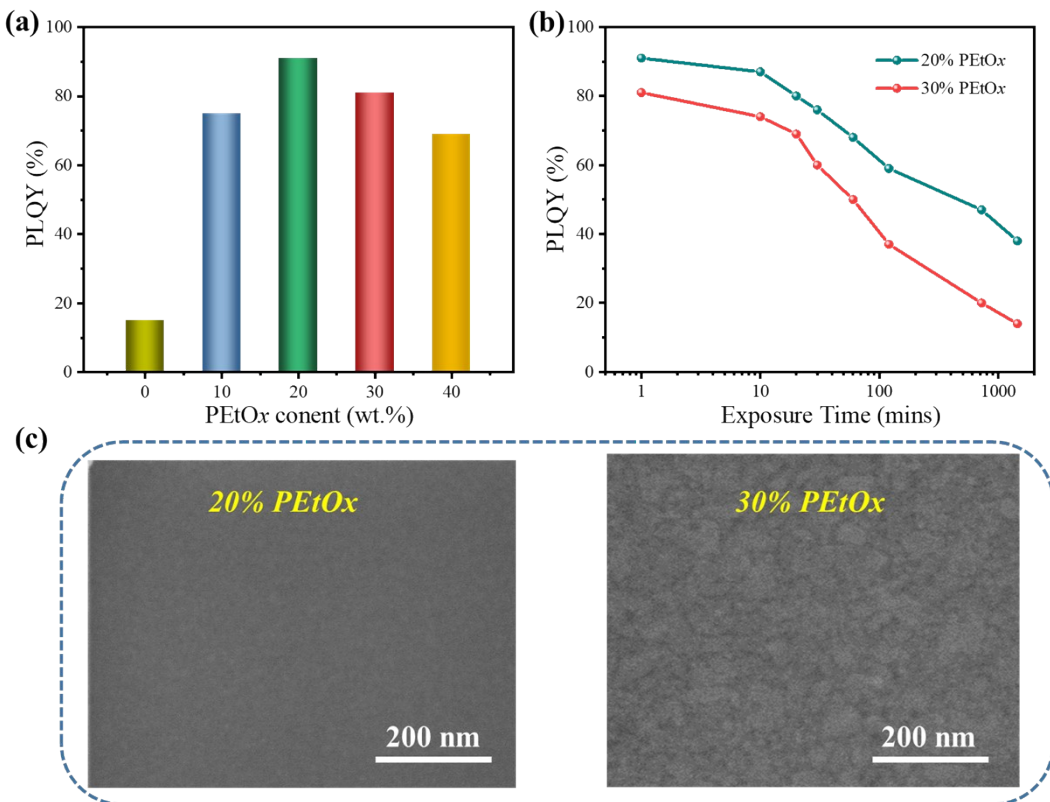


Figure S4. The relationship between the PLQY (a) and stability (b) of PBABr/CsPbBr_{0.6}I_{2.4}/PEtOx composite thin films and the PEtOx doping amount. (c) SEM images of the PBABr/CsPbBr_{0.6}I_{2.4}/PEtOx composite thin films with 20% and 30% PEtOx, respectively.

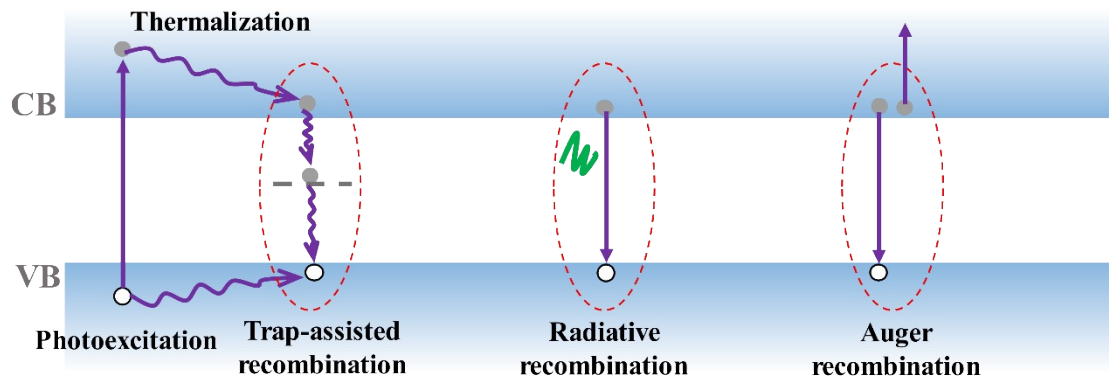


Figure S5. Schematic diagram of different recombination dynamics in perovskites.

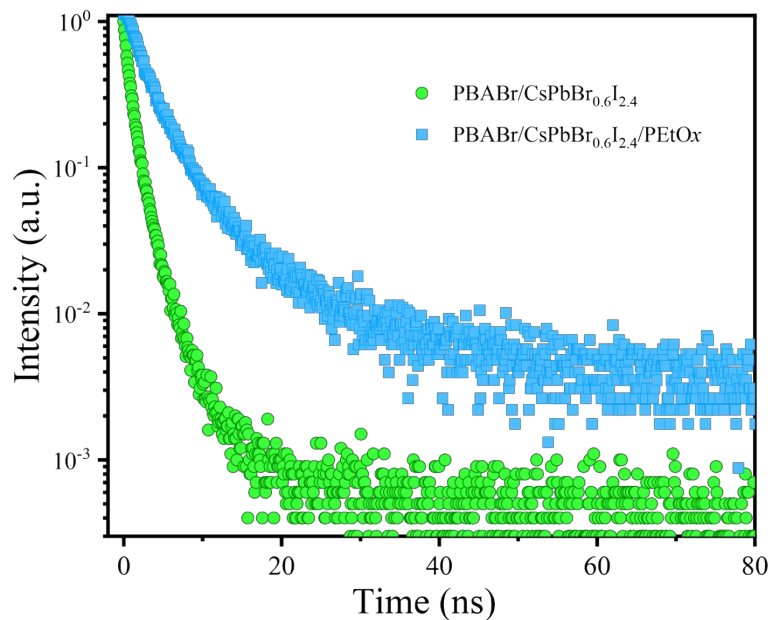


Figure S6. TRPL spectra of PBABr/CsPbBr_{0.6}I_{2.4} and PBABr/CsPbBr_{0.6}I_{2.4}/PEtO_x thin films under extremely low carrier density. The effective lifetime is 7.47 ns and 2.72 ns for PBABr/CsPbBr_{0.6}I_{2.4}/PEtO_x and PBABr/CsPbBr_{0.6}I_{2.4}, respectively. Under low carrier density ($\sim 10^{12} \text{ cm}^{-3}$), the bimolecular recombination and Auger recombination are inappreciable, and the monomolecular recombination constant k_1 can be obtained through the equation ($\tau_{1/e} = 1/(k_1 + k_2 * n/2 + k_3 * n^2/3)$).^[10]

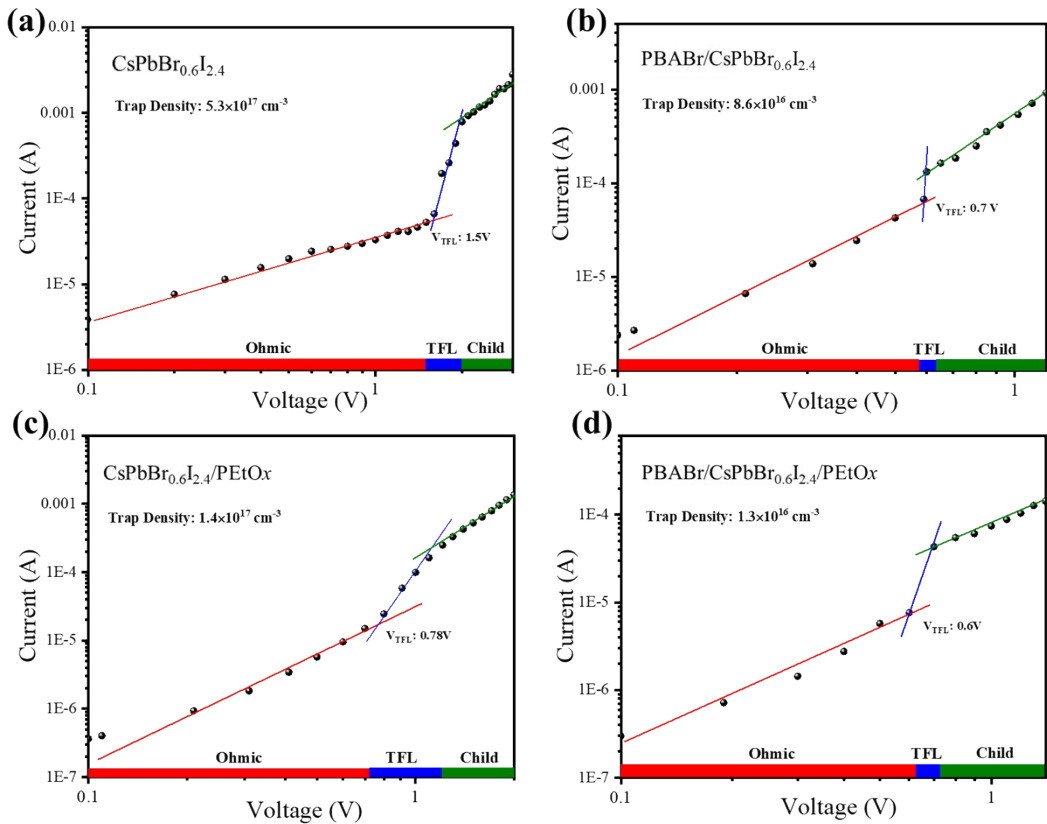


Figure S7. Trap density extraction of $\text{CsPbBr}_{0.6}\text{I}_{2.4}$ thin films with different additives by dark current-voltage measurement of hole-only devices with a device structure of ITO/PEDOT:PSS/Perovskite/ MoO_3/Ag .

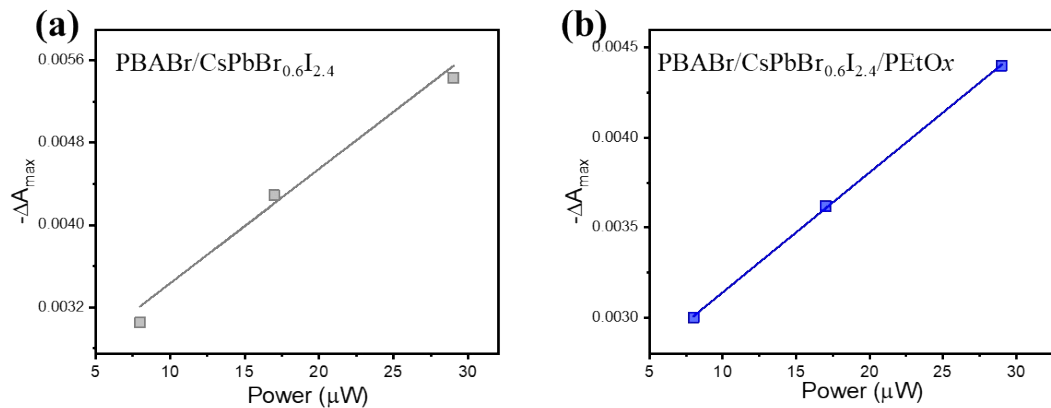


Figure S8. Transient absorption spectra. Initial TA bleach signal plotted over pump power for thin film PBABr/CsPbBr_{0.6}I_{2.4} (a) and thin film PBABr/CsPbBr_{0.6}I_{2.4}/PEtOx (b), which indicate they are in the unsaturated absorption region.

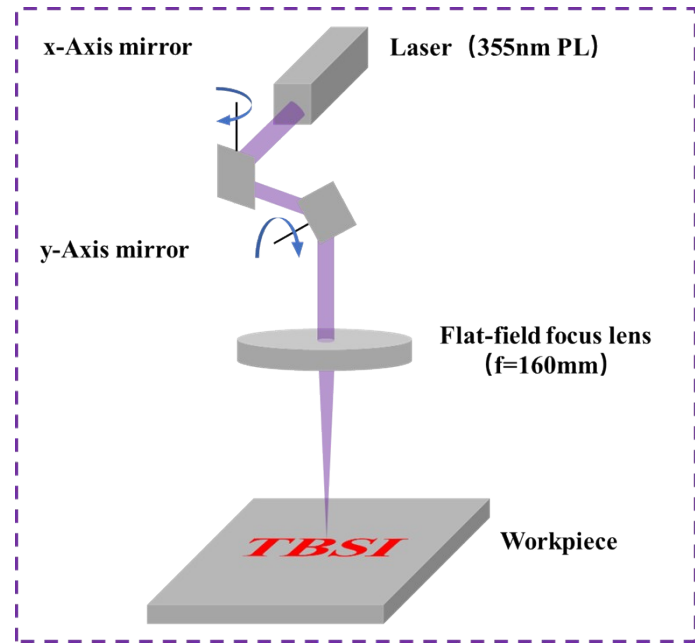


Figure S9. The detailed laser direct-write patterning setup.

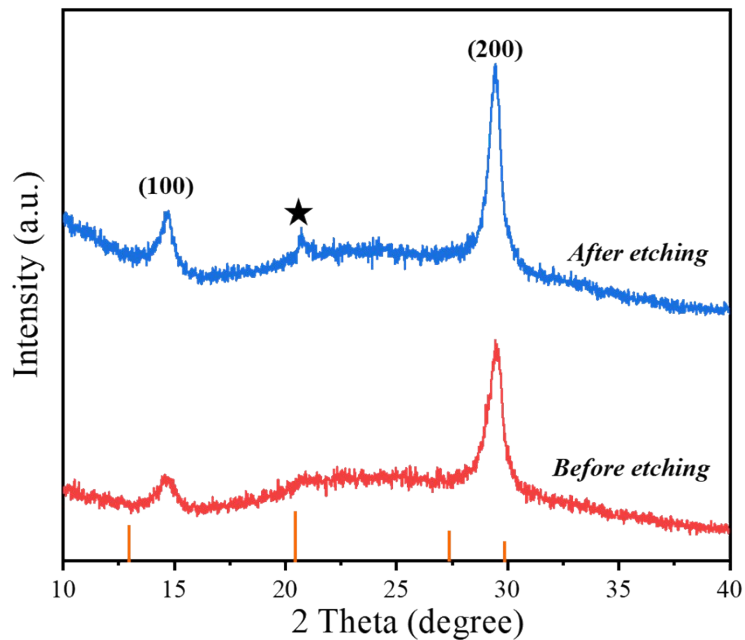


Figure S10. XRD patterns of perovskite films before and after laser etching.

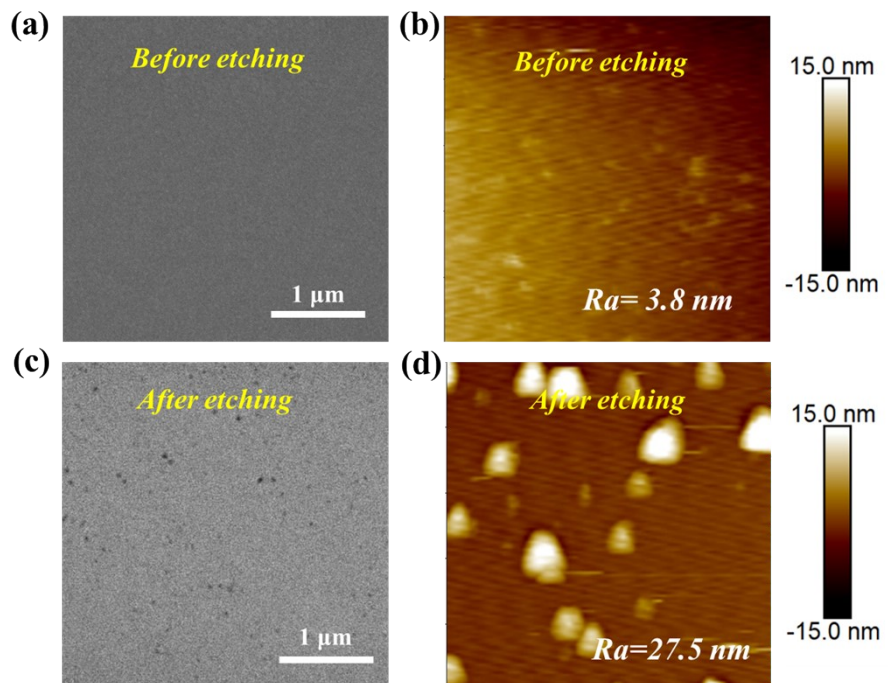


Figure S11. SEM and AFM images of perovskite thin films before (a, c) and after (b, d) laser etching.

References

- [1] Y. Hassan, O. J. Ashton, J. H. Park, G. Li, N. Sakai, B. Wenger, A. A. Haghhighirad, N. K. Noel, M. H. Song, B. R. Lee, R. H. Friend, H. J. Snaith, *J. Am. Chem. Soc.* **2019**, *141*, 1269-1279.
- [2] J. N. Yang, Y. Song, J. S. Yao, K. H. Wang, J. J. Wang, B. S. Zhu, M. M. Yao, S. U. Rahman, Y. F. Lan, F. J. Fan, H. B. Yao, *J Am Chem Soc* **2020**, *142*, 2956-2967.
- [3] J. Zhang, L. Zhang, P. Cai, X. Xue, M. Wang, J. Zhang, G. Tu, *Nano Energy* **2019**, *62*, 434-441.
- [4] H. Wang, Y. Dou, P. Shen, L. Kong, H. Yuan, Y. Luo, X. Zhang, X. Yang, *Small* **2020**, *16*, 2001062.
- [5] Y. Hassan, J. H. Park, M. L. Crawford, A. Sadhanala, J. Lee, J. C. Sadighian, E. Mosconi, R. Shivanna, E. Radicchi, M. Jeong, C. Yang, H. Choi, S. H. Park, M. H. Song, F. De Angelis, C. Y. Wong, R. H. Friend, B. R. Lee, H. J. Snaith, *Nature* **2021**, *591*, 72-77.
- [6] Y. Tian, C. Zhou, M. Worku, X. Wang, Y. Ling, H. Gao, Y. Zhou, Y. Miao, J. Guan, B. Ma, *Adv. Mater.* **2018**, *30*, 1707093.
- [7] L. Yang, Y. Zhang, J. Ma, P. Chen, Y. Yu, M. Shao, *ACS Energy Letters* **2021**, *6*, 2386-2394.
- [8] Z. Wang, F. Wang, B. Zhao, S. Qu, T. Hayat, A. Alsaedi, L. Sui, K. Yuan, J. Zhang, Z. Wei, Z. Tan, *J. Phys. Chem. Lett.* **2020**, *11*, 1120-1127.
- [9] F. Yuan, X. Zheng, A. Johnston, Y. Wang, C. Zhou, Y. Dong, B. Chen, H. Chen, J. Fan, G. Sharma, *Sci. Adv.* **2020**, *6*, eabb0253.
- [10] G. Xing, B. Wu, X. Wu, M. Li, B. Du, Q. Wei, J. Guo, E. K. Yeow, T. C. Sum, W. Huang, *Nat. Commun.* **2017**, *8*, 14558.